Upwellings along the Coasts of Somalia and Arabia

O. Carvalho Junior

Instituto Ekko Brasil

ABSTRACT

Background: Several authors have pointed out the relationship between seasonal changes of atmospheric winds, phytoplankton distribution and productivity in the Arabian Sea. The best example of such interaction is the western Arabian Sea region, which presents a large seasonal variation in temperature and chlorophyll because of the monsoons throughout the year. The main feature in the area is the strong western boundary current along the Somali and Arabian Peninsula coasts, which, with favorable winds, result in two important upwellings during the SW Monsoon. This work presents a characterization of the surface of the mixed layer along the Somali and Arabian coasts, based on temperature/salinity time diagram (TS-time diagram), temperature/ chlorophyll time diagram (TC-time diagrams) and harmonic analysis techniques.

Keywords: productivity; harmonic analysis; Arabian Sea; Indian Ocean.

Classification: FOR CODE:040699

Language: English

London Journals Press

LJP Copyright ID: 925641
Print ISSN: 2631-8490
Online ISSN: 2631-8504

London Journal of Research in Science: Natural and Formal

Volume 22 | Issue 1 | Compilation 1.0

Upwellings along the Coasts of Somalia and Arabia

O. Carvalho Junior

ABSTRACT

Background: Several authors have pointed out the relationship between seasonal changes of atmospheric winds, phytoplankton distribution and productivity in the Arabian Sea. The best example of such interaction is the western Arabian Sea region, which presents a large seasonal variation in temperature and chlorophyll because of the monsoons throughout the year. The main feature in the area is the strong western boundary current along the Somali and Arabian Peninsula coasts, which, with favorable winds, result in two important upwellings during the SW Monsoon. This work presents a characterization of the surface of the mixed layer along the Somali and Arabian coasts, based on temperature/salinity time diagram (TS-time diagram), temperature/ chlorophyll time diagram (TC-time diagrams) and harmonic analysis techniques.

Materials and Methods: Geographic distribution of amplitudes and phases of harmonic waves are generated for the chlorophyll, temperature, and salinity data, which are computed for an average year over a 5-degree grid along the Somali and Arabian coasts. They are based on the World Ocean Atlas Data Set and the AVHRR MCSST and CZCS phytoplankton pigment concentration data set. This classification includes the analysis of the annual and semi-annual amplitudes, plus multiple regression analysis between temperature, salinity, chlorophyll, Ekman pumping, components of the pseudo-stress wind and net-down- fresh-water-flow (ndff). To clarify the processes currently involved with the surface water properties, sea surface temperature (SST), sea surface salinity (SSS) and sea surface chlorophyll (SSC) are treated as pseudo-harmonic terms.

Results: TC-time diagrams show the upwelling along the Arabian and Somali coasts. Two peaks of low temperature are observed during the Northeast and Southwest Monsoons. The highest chlorophyll concentration and low temperature are related to the upwelling that occurs in these areas during the SW Monsoon. The chlorophyll bloom starts in May and declines in October. The maximum chlorophyll values occur during August, when temperatures are close to 24 °C. Comparing the TC-time and TS-time diagrams for the same area, it can be observed that the highest chlorophyll concentration from the TC-time diagrams, during the SW Monsoon, is not only related to a low temperature, but also to low salinity values. The meridional component of pseudostress wind and wind magnitude play a major role on temperature variability along the Arabian coast, during the SW Monsoon.

Conclusion: The application of time diagram technique has successfully identified the upwelling and the Arabian Sea Surface Water (ASSW) along Arabian and Somali coasts, as well as the geographical distribution of the seasonal cycles of temperature, salinity, and chlorophyll.

Keyword: productivity; harmonic analysis; Arabian Sea; Indian Ocean.

Author: Oldemar Carvalho Junior, Instituto Ekko Brasil - Research & Project Office.

I. INTRODUCTION

The relationship between seasonal changes of atmospheric winds, phytoplankton distribution and productivity in the Arabian Sea has been pointed out by several authors (Desai, 1992; Vase et al., 2018; Guieu et al., 2019; Smitha et al., 2022). The best example of such interaction is the

western Arabian Sea region, which presents a large seasonal variation in temperature and chlorophyll because of the monsoons throughout the year. During the SW Monsoon, a strong current flow northward along the western boundary of the Arabian Sea, originating the upwellings along the Somali and Arabian coasts. During the NE Monsoon, a weak anticyclone replaces the strong northward flow from the SW Monsoon (Figure 1). The air-sea interface represents a common boundary shared by the ocean and atmosphere. Solar radiation, wind stress, Ekman pumping, heat exchange, among other atmospheric and oceanographic processes, result in large seasonal and inter-annual variability of the water properties at the ocean surface.

The main feature in the area is the strong western boundary current along the Somali and Arabian Peninsula coasts, which, with favorable winds, result in two important upwellings during the SW Monsoon. This work establishes a systematic classification of the two upwellings that occur along the Somali and Arabian coasts, based on averages and standard deviations of TS and TC time diagrams for each 5° square. This classification includes the analysis of the annual and semi-annual amplitudes, plus multiple regression analysis between temperature, salinity, chlorophyll, Ekman pumping, components of the pseudo-stress wind and net-down-fresh-water-flow (ndff). The annual cycle of SST, SSS, and SSC are treated as a simple harmonic term as it tends to be repeated in a regular cycle. This annual oscillation, however, can be the product of opposing influences, for example the two phases of the monsoons in the Indian Ocean. It is not very common to find harmonic analysis in the oceanographic literature but some authors (Unnikrishnan et al., 1997; Clarke and Liu, 1993; Levi's, 1987) have introduced the sub-harmonic six-monthly term to deal with the perturbations observed in the oceanic mixed layer.

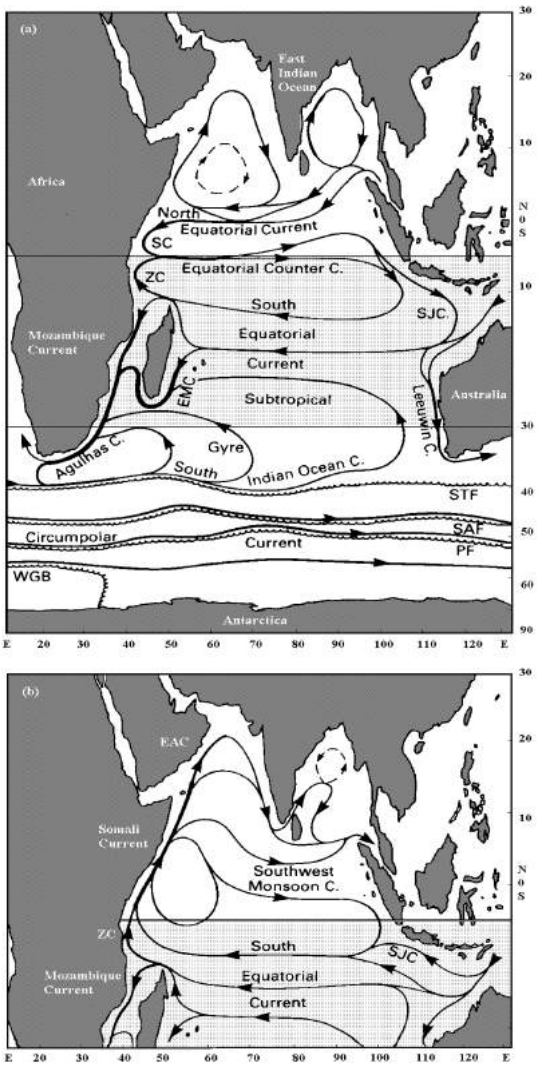

Figure 1: Surface currents in the Indian Ocean. (a) NE Monsoon (Dec-April); (b) SW Monsoon (Jun-Oct). EAC = East Arabian Coast; SJC = South Java Current; ZC = Zanzibar Current; EMC = East Madagascar Current; SC = Somali Currents; STF = Subtropical Front; SAF = Sub-Antarctic Front; PF = Antarctic Polar Front; WGB = Weddell Gyre Boundary. Adapted from Tomczak and Godfrey (1994).

These analyses reveal different physical processes related to the temperature, salinity, and chlorophyll variability. The variability of these variables, represented by the diagrams, can then be related to a kind of water mass and upwellings at the ocean's surface. The application of the classic TS-diagrams (curves) is because similar water masses are expected to present similar TS-curves. Therefore, a collection of TS-curves, for a given region or ocean, can provide information on the distribution and structure of the water masses in the water column. Similar methodology is applied in the present work using TS-time and TC-time diagrams. A time diagram plots the variables (temperature, salinity, and chlorophyll) for a given location or region as a function of time (e.g., over a period of one year).

II. MATERIAL AND METHODS

The Methodology is based on the application of TS-time and TC-time diagrams. A time diagram plots the variables (temperature, salinity, and chlorophyll) for a given location or region as a function of time (e.g., over a period of one year). The observations of sea surface temperature, sea surface salinity and sea surface chlorophyll lie on a line that connects 12 points (months). Each point (month) can be seen as a water type in which the mixing, diffusion, and intensity of the

interaction between different physical process result in different surface distribution of temperature, salinity, and chlorophyll. Therefore, these 12 water types can be seen as representing the time history of the influence of different factors such as wind regime, rainfall distribution, drainage area, heat budget and balance between precipitation and evaporation.

The temperature and salinity data for the ocean surface for each 5° square are obtained from the *World Ocean Atlas Data Set* (1994). Chlorophyll concentrations for the ocean's surface are calculated from data originated by sensors of the *AVHRR MCSST* and *CZCS* satellites. The harmonic terms are considered to be stationary, as the averages and corresponding correlations are not expected to vary significantly in a long period of time. In this way, Fourier series can then express the stationary time series symbolically as a cosine function in which the first and second harmonic terms are multiplied by the maximum amplitude of the variable and added to the mean annual parameter. The modelled data can thus be expressed as:

$$O(t) = O + cos\left(\omega_a \times t - a\right) + B \times cos\left(\omega_s \times t - b\right)$$

where: $O(t)$ = observed value as a function of time where t is time in days, since the start of an arbitrary year, $\overline{O}$ = mean value over the period, A = Amplitude of the annual harmonic component, B = Amplitude of the semi-annual harmonic component, a = Phase-lag of the annual component, b = Phase-lag of the semi-annual component, ω_a = Angular frequency $2\pi/365.25$ which represents the increment in phase per unit time, t, of the annual harmonic component, ω_s = ditto for the semi-annual component but $2\pi/182.62$, ω_a x t - a = phase of the annual harmonic, π, ω_s x t - b = phase of the semi-annual harmonic.

O represents the average annual temperature, salinity, or chlorophyll, and is a positive constant. The amplitude value (A *or* B) represents the motion, oscillating within a range of + or -. Phase-lag is expressed in degrees and increments at 30° per month for the first harmonic and 60° per month for the second. It expresses the average time when the maximum of the value occurs within the annual cycle.

The TS-time diagrams, expressed as normalized temperature and salinity, show the influence of the temperature in the definition of the water mass. As temperature and salinity exhibit different units and are then difficult to be compared, they will be normalized in terms of thermal expansion and salinity contraction coefficients, respectively. The application of a normalized temperature/salinity ratio, together with the amplitude ratio of the semiannual and annual harmonic terms, resulted in an improvement of the discrimination of the first and second harmonic components as a basis of characterization.

Least square procedure is performed for the upwellings areas to determine the main factors affecting the variables. The multiple regression model is performed for each 5 square degrees of the study area, considering the Standard Multiple Regression of components of pseudo-stress wind (Wx = zonal; Wy = meridional), wind magnitude (Wmg), Ekman pumping and net-down-freshwater-flux (ndff).

In this study, geographic distribution of amplitudes and phases of harmonic waves are generated for the chlorophyll, temperature, and salinity data, which are computed for an average year over a 5-degree grid along the Somali and Arabian coasts. The former provides a century-long record of temperature and a seventy-year record of salinity. The latter documents temperature and phytoplankton for the time intervals 1981-1986 and 1978-1986, respectively.

III. RESULTS

During the Northeast Monsoon, the wind is oblique to the coastline (40 to 50 degrees northeast) whereas during the Southwest Monsoon it is parallel (150 to 220 degrees southwest) (Figure 2). It can be observed a lack of

time between the beginning of the favorable conditions and the chlorophyll growth (from May to September).

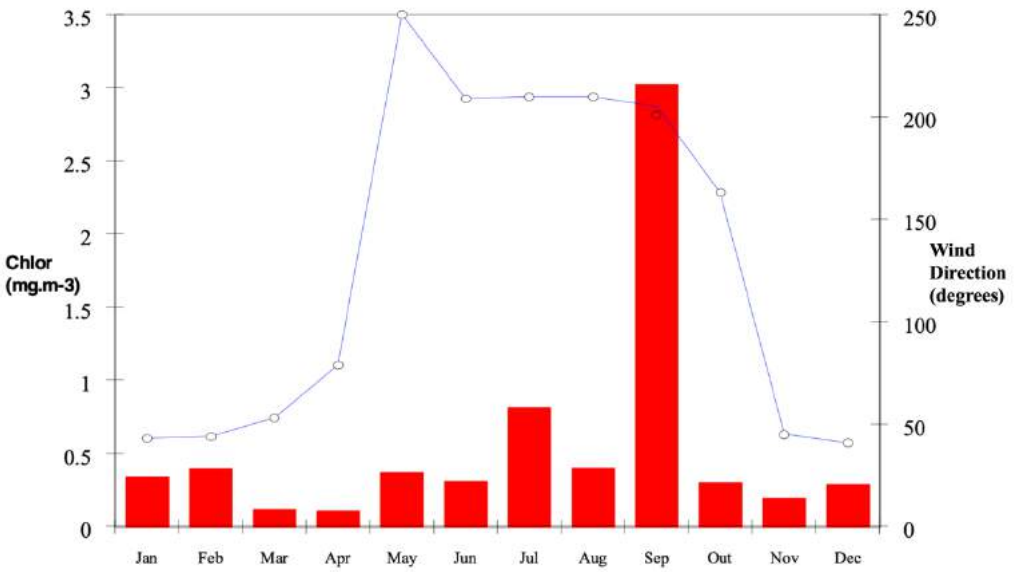

Figure 2: Seasonal variation in wind direction and chlorophyll concentration at the Somali coast.

The higher temperature variability during May-June-July and August-September-October reveals the influence of strong winds, which are observed during the Southwest Monsoon along the Somali coast. The long 'lag-time' interval between May and September may be reflecting a delay in the transport of nutrients to the euphotic zone. The highest chlorophyll concentration and low temperature are related to the upwelling that occurs in these areas during the SW Monsoon. The chlorophyll bloom starts in May and declines in October. The maximum chlorophyll values occur during September, when temperatures are close to 24 °C.

The upwelling at the Arabian coast presents higher salinities (from 35.8 psu to 36.2 psu) than at the Somali coast (from 35.4 psu to 35.7 psu) (Figure 3). The TS-time diagrams exhibit a bimodal pattern for temperature and salinity, with two maximum and two minimum for a year. The TC-time diagrams show the upwelling along the Arabian and Somali coasts. Two peaks of low temperature are observed during the Northeast and Southwest Monsoons, during January/February, the peak of the NE Monsoon, and August, the peak of the SW Monsoon. A maximum temperature is observed during May (close to 30 °C) and a secondary maximum during October/November (around 28 °C), the transition between NE to SW Monsoon, when wind magnitude is close to zero. The TC-time diagram for the western Arabian Sea points out the contrast in productivity between the SW Monsoon and NE Monsoon, as a result of upwellings that occur during August and September. The maximum chlorophyll concentration occurs from July to September, with a maximum peak during September (0.81 $mg.m^3$). This chlorophyll maximum can be associated with a decrease in temperature during August (25.77 °C).

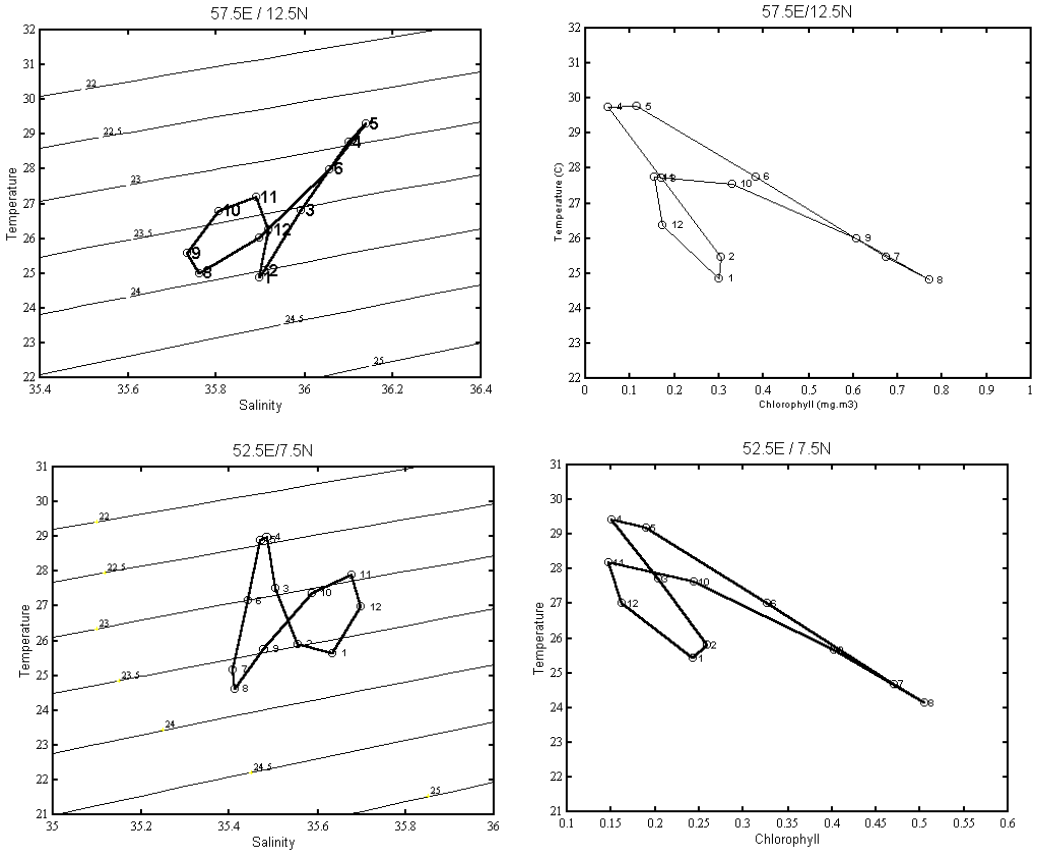

Figure 3: Distribution of sea surface properties for the Arabia (57,5 E/12,5 N) and Somali (52,5 E/7,5 N) upwellings. TS-time and TC-time diagrams relative to each upwelling area.

Figure 4 exhibits the normalized temperature and salinity time diagrams for each upwelling region (Arabian and Somali upwellings). They show that temperature plays a major role in the shape of the TS-time diagrams for both areas. For example, at the Somali coast (right diagram) αT ranges from 0.0073 to 0.0095 (22 units) while βS changes from 0.0261 to 0.0263 (only 2 units). A similar situation is observed along the Arabian coast (left diagram) where αT changes from 0.0072 to 0.0095 (23 units) and βS from 0.0265 to 0.0267 (only 2 units).

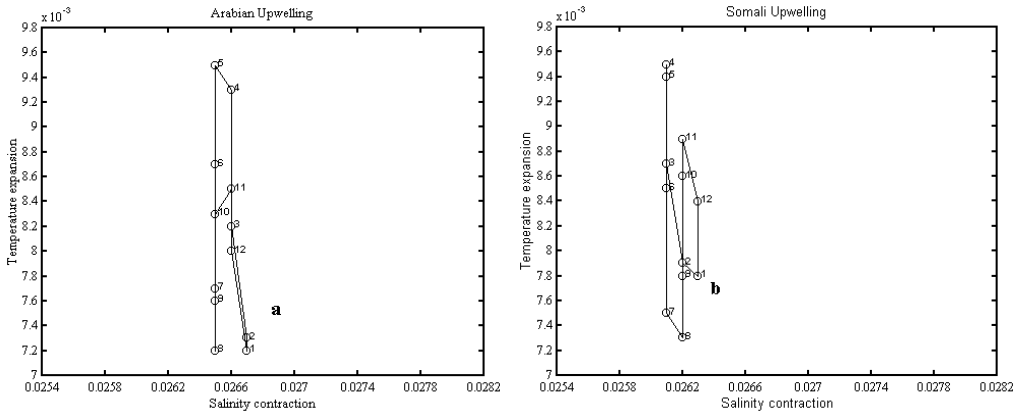

Figure 4: Normalized TS-time diagrams at Arabian coast 57.5° E/17.5° N (left diagram) and Somalian 52.5° E/7.5° N (right diagram).

Along the Somali and Arabian coasts, the meridional component of pseudostress wind (Wy) and wind magnitude (Wmg) reaches maximum speed (close to 15 $m.s^{-1}$) during the period of June until August, when temperature decreases to a minimum of 24 °C. Winds start to become gradually weaker from July (~15 $m.s^{-1}$) to October (close to zero) when temperature increases from about 24 °C (July/August) to around 28 °C (November). The increase in temperature represents the interruption of cold and nutrient rich water supply from below to the surface. Temperature variability along the Arabian coast, during the SW Monsoon, exhibits and adjusted R^2 of 0.914 (91%) as a result of ndff, Wmg and Wy, in which Wmg and Wy play a major role.

The variables ndff and both components of pseudostress wind represent 83% of the variability in chlorophyll, in which Wx and Wy are more effective than ndff by a factor of 3 and 4, respectively. The significance of the wind and Ekman pumping along the Arabian coast is not surprising, as upwellings are closely dependent on favorable winds that blow along the coastline.

The maximum chlorophyll concentration occurs from July to September, with a maximum peak during September. This chlorophyll maximum can be associated with a decrease in temperature during August (25.77 °C). Comparing the TC-time and TS-time diagrams for the same area, it can be observed that the highest chlorophyll concentration from the TC-time diagrams, during the SW Monsoon, is not only related to a low temperature, but also to low salinity values. The variables ndff and both components of pseudostress wind represent 83% of the variability in chlorophyll, in which Wx and Wy are more effective than ndff by a factor of 3 and 4, respectively.

The least square method shows that 69% (adjusted R^2) of salinity variability, during the SW Monsoon, can be exclusively explained by Ekman pumping. The adjusted R^2 falls to 39% for the Arabian Sea where Ekman, wind magnitude and zonal component of pseudostress wind account for salinity variability during the same period. During the NE Monsoon, a significant adjusted R^2 of 96%, for salinity, is obtained only for the Somali region, where wind magnitude, Wy and ndff affect salinity predominantly.

IV. DISCUSSION

During the Southwest Monsoon, the parallel direction of the wind causes an offshore wind induced transport. The upwelling replaces the warm surface water with cold and nutrient rich waters, therefore increasing the productivity in the area. The lack of time between the beginning of the favorable conditions and the chlorophyll growth is commonly known as 'lag time'. This phenomenon is related to the physiology of the organism itself, such as biochemical adjustment and external factors (nutrient, light limitation and grazing). The 'lag-time' interval on chlorophyll growth represents an adjustment of the environment changes (Habeebrehman et al., 2008; Al-Azri et al., 2010). Negative environmental conditions for the phytoplankton population can act as a barrier between the phytoplankton and the nutrients. The long interval observed from the beginning of favorable winds (May), along the coast of Somalia, until the peak of chlorophyll concentration (September) may also be related to a combination of limiting factors.

The bimodal pattern of the TS-time diagrams for the ASSW, is a result of the reversal of the wind stress and the occurrence of upwellings. The temperature minimum observed during the NE Monsoon is related to the annual solar path and evaporative cooling. The temperature minimum that occurs during the SW Monsoon is associated with evaporative cooling and upwellings along the Somali and Arabian coasts. The two maximums of temperature occur during the transition of the monsoons, when wind magnitude decreases, thus resulting in a decrease of evaporative cooling at the surface. The contrast in productivity between the SW Monsoon and NE Monsoon is a result of upwellings that occur during August and September. The maximum chlorophyll concentration occurs from July to September, with a maximum peak during September (0.81 $mg.m^3$). This chlorophyll maximum can be

associated with a decrease in temperature during August (25.77 °C).

The rising temperature is interrupted in November and then starts to decrease again to around 26 °C (January/February) as the wind shifts direction from northward to southward and from eastward to westward. The evaporation, as a result of the strength of the wind during the NE Monsoon, with the decrease in solar radiation (northern winter) on the surface result in lost of heat to the atmosphere. At the Somali area, this situation is combined with a small upwelling during the NE Monsoon.

As can be seen from the *alphaT* and *BetaS* time diagrams, temperature plays a major role in the shape of the TS-time diagrams for the upwelling areas of Somali and Arabian coasts. The decrease of temperature with increasing chlorophyll at the sea surface can be clearly observed when analyzing the TC-time diagram.

During the NE Monsoon, a significant adjusted R^2 of 96%, for salinity, is obtained only for the Somali region, where wind magnitude, Wy and ndff affect salinity predominantly. High salinities are related to SW winds, which bring waters from the north of the Arabian Sea. On the other hand, during the SW Monsoon low salinity is clearly associated with low temperature (24 °C), which endorses the influence of upwelling. The transport of AMMW low salinity waters through the South Equatorial Current towards the African coast and then northward by the Somali current could be an explanation for this low salinity values during the SW Monsoon. However, they do not explain the observed low temperatures.

An explanation of the influence of the upwelling upon the salinity can be found in Wyrtki (1973), who has reported the presence of a salinity minimum in the west equatorial region, between 100 and 500 m deep. This low salinity layer separates the high salinity water of the northern Indian Ocean from the high salinity water of the subtropical gyre. Leetmaa et al. (1982), based on vertical transects along the Somali coast during the onset of the SW Monsoon, also describes the presence of a lower salinity layer at about 150 m deep. Therefore, it is possible to conclude that the region along the Somali coast presents a vertical structure where a layer of high salinity water is positioned on the top of another layer of low salinity water. During the SW Monsoon, the upwelling process breaks this structure, bringing low salinity water to the surface. The low salinity values, associated with high concentration of chlorophyll and low temperature, seem to be a result of the characteristics of the subsurface water in the region.

The correlation between wind (Wy and Wmg) and salinity reflects, in part, the circulation pattern during the SW Monsoon. During this monsoon, the Somali current is intensified and fed by the South Equatorial Current and Zanzibar Current, with a strong northward flow. The South Equatorial Current pushes the high salinity water from the Arabian Sea further north, as can be seen from the isohaline of 36 in March, which shifted towards the north during August.

In summary, different causes can be attributed to the distribution pattern of chlorophyll concentration in the study area. During the Southwest Monsoon, chlorophyll concentrations are different along the Somali (0.5 $mg.m^{-3}$-1.4 $mg.m^{-3}$) and Arabian (3 $mg.m^{-3}$) regions. Shetye et al. (1994) and Banse and English (2000) pointed out the importance of the offshore transport mechanism that brings upwelled cold waters along the Arabian coast from 300 to 700 meters deep. During the Southwest Monsoon, the Somali, and East Arabian currents dominate the flow in the Arabian Sea with velocities between 0.5 to 0.8 m s^{-1} (Tomczak and Godfrey 1994). These currents flow northward along the Arabian coast and generate an offshore transport, which results in water convection from below the photic zone.

The circulation patterns around the Somali and Arabian coasts differ from season to season. During the Northeast Monsoon, the subtropical gyres, the north equatorial current, the equatorial counter current and the south equatorial current influence the region. During the Southwest Monsoon, the main oceanographic features along the equatorial region are the Southwest monsoon current and south equatorial current, which

present a westward flow. Therefore, it is expected the variation of salinity, temperature, and chlorophyll, in the western boundary of the Indian Ocean, to be influenced by a combination of factors such as the westward spreading of the low salinity Australasian Mediterranean Water along the equator and upwelling.

V. CONCLUSION

The western Arabian Sea represents a region too complex to be fully explained by a single treatment. The association of similar TS and TC-time diagrams result as a general method for water masses identification and diagnosis. However, it is important to point out the need of previous analysis (harmonic and regression techniques) to produce the modelled data and to corroborate the application of the TS and TC-time diagrams.

ACKNOWLEDGMENT

To Matthias Tomczak, a great friend who always manifested lucidity in a natural and instantaneous way, and who inspired my life and many others in the field of oceanography.

REFERENCES

1. Al-Azri, A. R., Piontkovski, S. A., Al-Hashmi, K. A., Goes, J. I., & do Gomes, H. R. (2010). Chlorophyll a as a measure of seasonal coupling between phytoplankton and the monsoon periods in the Gulf of Oman. *Aquatic Ecology*, *44*(2), 449–461.https://doi.org/10.1007/s10452-009-9303-2
2. Banse, K., & English, D. C. (2000). Geographical differences in seasonality of CZCS-derived phytoplankton pigment in the Arabian Sea for 1978–1986. *Deep Sea Research Part II: Topical Studies in Oceanography*, *47*(7), 1623–1677. https://doi.org/10.1016/S0967-0645(99)00157-5
3. Clarke, A. J., & Liu, X. (1993). Observations and Dynamics of Semiannual and Annual Sea Levels near the Eastern Equatorial Indian Ocean Boundary. *Journal of Physical Oceanography*, *23*(2), 386–399. https://doi.org/10.1175/1520-0485(1993)023<0386:OADOSA>2.0.CO;2
4. Desai, B. N. (1992). *Oceanography of the Indian Ocean*.https://drs.nio.org/xmlui/handle/2264/7348
5. Guieu, C., Al Azhar, M., Aumont, O., Mahowald, N., Levy, M., Ethé, C., & Lachkar, Z. (2019). Major Impact of Dust Deposition on the Productivity of the Arabian Sea. *Geophysical Research Letters*, *46* (12), 6736–6744. https://doi.org/10.1029/2019GL082770.
6. Habeebrehman, H., Prabhakaran, M. P., Jacob, J., Sabu, P., Jayalakshmi, K. J., Achuthankutty, C. T., & Revichandran, C. (2008). Variability in biological responses influenced by upwelling events in the Eastern Arabian Sea. *Journal of Marine Systems*, *74*(1), 545–560. https://doi.org/10.1016/j.jmarsys.2008.04.002
7. He, J., & Mahadevan, A. (2021). How the Source Depth of Coastal Upwelling Relates to Stratification and Wind. *Journal of Geophysical Research: Oceans*, *126*(12), e2021JC017621.https://doi.org/10.1029/2021JC017621
8. Lee, C. M., Jones, B. H., Brink, K. H., & Fischer, A. S. (2000). The upper-ocean response to monsoonal forcing in the Arabian Sea: Seasonal and spatial variability. *Deep Sea Research Part II: Topical Studies in Oceanography*, *47* (7), 1177–1226.https://doi.org/10.1016/S0967-0645(99)00141-1
9. Leetmaa, A., Quadfasel, D. R., & Wilson, D. (1982). Development of the Flow Field during the Onset of the Somali Current, 1979. *Journal of Physical Oceanography*, *12*(12), 1325–1342. https://doi.org/10.1175/1520-0485(1982)012<1325:DOTFFD>2.0.CO;2
10. Levitus, S. (1987). A Comparison of the Annual Cycle of Two Sea Surface Temperature Climatologies of the World Ocean. *Journal of Physical Oceanography*, *17*(2), 197–214. https://doi.org/10.1175/1520-0485(1987)017<0197:ACOTAC>2.0.CO;2
11. Shetye, S. R., Gouveia, A. D., & Shenoi, S. S. C. (1994). Circulation and water masses of the Arabian Sea. *Proceedings of the Indian Academy of Sciences - Earth and Planetary*

Sciences, *103*(2), 107–123. https://doi.org/10.1007/ BF02839532
12. Smitha, B. R., Sanjeevan, V. N., Padmakumar, K. B., Hussain, M. S., Salini, T. C., & Lix, J. K. (2022). Role of mesoscale eddies in the sustenance of high biological productivity in North Eastern Arabian Sea during the winter-spring transition period. *Science of The Total Environment*, *809*, 151173. https://doi.org/10.1016/j.scitotenv.2021.151173.
13. Tomczak, M., & Godfrey, J. S. (1994). *Regional Oceanography: An Introduction*. Pergamon.
14. Unnikrishnan, A. S., Prasanna Kumar, S., & Navelkar, G. S. (1997). Large-scale processes in the upper layers of the Indian Ocean inferred from temperature climatology. *Journal of Marine Research*, *55*(1), 93–115. https://doi.org/10.1357/ 0022240973224490
15. Vase, V. K., Dash, G., Sreenath, K. R., Temkar, G., Shailendra, R., Mohammed Koya, K., Divu, D., Dash, S., Pradhan, R. K., Sukhdhane, K. S., & Jayasankar, J. (2018). Spatio-temporal variability of physico-chemical variables, chlorophyll a, and primary productivity in the northern Arabian Sea along India coast. *Environmental Monitoring and Assessment*, *190*(3), 148. https://doi.org/10.1007/s10661-018-6490-0.
16. Vijith, V., Shetye, S. R., Gouveia, A. D., Shenoi, S. S. C., Michael, G. S., & Sundar, D. (2022). Circulation in the region of the West India Coastal Current in March 1994 hydrographic and altimeter data. *Journal of Earth System Science*, *131*(1), 16. https://doi.org/10.1007/s12040-021- 01761-5
17. Wyrtki, K. (1973). Physical Oceanography of the Indian Ocean. In B. Zeitzschel & S. A. Gerlach (Eds.), *The Biology of the Indian Ocean* (pp. 18–36). Springer. https://doi.org/10.1007/978 -3-642-65468-8_3